ADVANCED BIOLOGY
www.advanced-bio.com

Establishment and Characterization of Single and Triple-Agent Resistant Osteosarcoma Cell Lines

*Kaan Low, Frank Hills, Helen C. Roberts, and Britta Stordal**

Two human osteosarcoma cell lines (MG-63 and HOS-143B) are developed into drug-resistant models using a short-term drug exposure and recovery in drug-free media. Cisplatin, doxorubicin, and methotrexate are used as single agents and in triple combination. The highest level of resistance to cisplatin is observed in MG-63/CISR8, doxorubicin in HOS-143B/DOXR8, and methotrexate in HOS-143B/MTXR8. The MG-63/TRIR8 and HOS-143B/TRIR8 triple-resistance models show lower levels of resistance to combination treatment and are not resistant to the drugs individually. Apoptosis assays suggest that the resistance in MG-63/TRIR8 isfrom cisplatin and methotrexate and not doxorubicin. In contrast, the resistance in HOS-143B/TRIR8 is from doxorubicin and methotrexate instead of cisplatin. Upregulation of P-glycoprotein is seen in all resistant models except those developed with single-agent methotrexate. However, P-glycoprotein is not causing resistance in all cell lines as the inhibitor elacridar only reverses the resistance of doxorubicin on MG-63/DOXR8 and HOS-143B/TRIR8. The migration of the MG-63 resistant models is significantly increased, their invasion rate tends to increase, and RT-PCR shows a switch from epithelial to mesenchymal gene signaling. In contrast, a significant decrease in migration is seen in HOS-143B resistant models with their invasion rate tending to decrease and a switch from mesenchymal to epithelial gene signaling.

1. Introduction

Osteosarcoma is a rare malignant bone tumor that occurs primarily in adolescents and young adults.[1] It is highly metastatic and the lungs are the most common site of metastases.[2,3] Prior to the adoption of chemotherapy in the mid-1970s, more than 85% of post-surgery osteosarcoma patients developed metastasis.[4] Nowadays, standard osteosarcoma treatment of osteosarcoma includes neo-adjuvant chemotherapy followed by surgical removal and adjuvant multi-drug chemotherapy.[5,6] The combination of cisplatin (CIS), doxorubicin (DOX), and high-dose methotrexate (MTX) is the standard treatment for most patients. Surgery combined with chemotherapy has improved the survival rate for osteosarcoma patients to 60–70%.[7] However, most patients with metastatic or recurrent osteosarcoma have poor prognosis due to the development of chemotherapeutic drug resistance.[8,9]

One of the methods to improve the survival rate of osteosarcoma patients is by overcoming chemotherapy resistance.[10] The development of drug resistance in osteosarcoma has been studied and several mechanisms demonstrated, including genetic alterations,[11] drug-target mutation and amplification,[12] altered drug accumulation,[13] and autophagy.[14] The expression of the gene MDR1, which is responsible for producing P-glycoprotein (P-gp), has been widely studied in osteosarcoma.[15,16] P-gp is a membrane-bound protein which transports doxorubicin and methotrexate out from the cells, leading to chemoresistance.[17,18]

Developing drug-resistant cancer cell models is a useful approach to study the mechanisms of chemoresistance in cancer cells. Previous resistant models have been established by using osteosarcoma cell lines such as SOSP-9607,[19] Saos-2,[20] MG-63,[21] and U-2OS.[22] These established osteosarcoma resistant models have increased fold resistance ranges from 6 to 120-fold compared to their parental cell lines.[19–22] They also exhibit cross-resistance to other chemotherapeutic drugs including ifosfamide, epidoxorubicin, pirarubicin, and paclitaxel.[19–22]

In the present study, clinically relevant chemo-resistant osteosarcoma cell models were developed from the cell lines MG-63 and HOS-143B. MG-63 was established from a 14-year old male with marginally metastatic osteosarcoma;[23] and HOS-143B originally derived from HOS, was established from a 13-year old Caucasian female with significant metastatic characteristics.[24] Chemo-resistant models of MG-63 and HOS-143B were developed by using a pulsed-selection strategy where cells were incubated with constant concentration of chemotherapeutic drugs for 72 h and then allowed to recover in drug-free media. The purpose of this method is to simulate a similar experience with osteosarcoma patients who undertake clinical chemotherapy treatment; and therefore, this is a clinically

K. Low, F. Hills, H. C. Roberts, B. Stordal
Department of Natural Sciences
Middlesex University London
Hendon, London NW4 4BT, UK
E-mail: b.stordal@mdx.ac.uk

The ORCID identification number(s) for the author(s) of this article can be found under https://doi.org/10.1002/adbi.202200194.

DOI: 10.1002/adbi.202200194

relevant osteosarcoma resistant model. This study is the first to use a multi-drugs combination approach as the selection strategy, where CIS, DOX, and MTX were mixed as a single treatment. The aim of this study was to develop a novel drug-resistant model by using a combination of drugs instead of a single drug as shown in previously established models.[19–22] We hypothesized that cells receiving the combination treatment would develop resistance slower or at a lower level compared to a single-agent treatment.

2. Results

2.1. Sensitivity Profile

The baseline resistance (IC_{50}) value of HOS-143B is higher when treated with single agent cisplatin ($p = 0.0002$) and methotrexate ($p = 0.012$) compared to MG-63 (**Table 1**). In contrast, MG-63 displayed a higher baseline resistance to single-agent doxorubicin ($p = 0.001$) (Table 1). The sensitivity profile of MG-63 and HOS-143B for the combination of drugs was also determined by performing the cytotoxicity assay with the mixture of CIS, DOX, and MTX. The baseline resistance of each drug within the combination of drugs is included in Table 1 for MG-63 (TRI) and HOS-143B (TRI). All drugs are combined in the cytotoxicity assay, and the values are the IC_{50} of the individual agents in the combination.

2.2. Dose Optimization

Doses of cisplatin, doxorubicin, and methotrexate were first selected within the range of IC60–IC90 to achieve the elimination of nearly 60–90% of the cell density after 3 days of drug incubation followed by growth to confluence after drug exposure. The doses were used in trials and were then optimized by either increasing or decreasing depending on the response of the cell lines. From the recovery plots **Figure 1**A,B show that recovery from cisplatin, doxorubicin, and methotrexate differed from each other. In MG-63, the recovery time was shortest when treated with methotrexate and combination of drugs and followed by cisplatin and doxorubicin (Figure 1A). In HOS-143B, the recovery time was shortest when treated with combination of drugs, followed by cisplatin, methotrexate, and doxorubicin (Figure 1B). The specific dose of each drug, including single agents and triple-combination, was selected after two rounds of optimization as shown in Figure 1 and was used for developing the resistance models.

2.3. Recovery

Generally, all sublines required less time to recover as the rounds of selection increased. The recovery plots are shown in Figure 1C,D grouped per ascending rounds of selection for MG-63 and HOS-143B. The recovery rate of the HOS-143B subline treated with cisplatin showed a greater difference between rounds of selection compared to the MG-63 subline. The HOS-143B subline treated with the triple-combination of drugs recovered quicker overall compared to those treated with the single agents.

2.4. Fold Resistance

The fold resistance of each subline was measured at weekly intervals for 3-weeks after each round of selection (Figure 1E–H). Most of the sublines developed resistance over the course of treatments. Fold resistances increased from round to round except for the MG-63 subline treated solely with doxorubicin (Figure 1F). Figure 1E–G shows the extent of resistance development after eight rounds of selection for single-agent cisplatin, doxorubicin, and methotrexate treatments in MG-63 and HOS-143B sublines. This was examined to investigate whether osteosarcoma cells with higher metastatic potential (HOS-143B) would develop drug resistance earlier cells with lower metastatic potential (MG-63).[25,26] We found that both cells with different degree of metastatic potential behaved similarly in developing resistance; higher levels were observed to cisplatin and methotrexate in both models. Figure 1H shows the results of fold resistance after eight rounds of selection for the triple combination of drugs.

2.5. Cell Morphology

Morphology of the resistant models was observed by light microscopy (**Figure 2**) and analyzed with ImageJ (**Figure 3**). Some of the resistant cell lines had a decrease in cell size compared to their parental cell line; this effect was consistent in both cisplatin-resistant models. All of the resistant cell lines showed a decrease in cell circularity associated with a shift to

Table 1. IC_{50} values of parental cell lines treated with single-agent and triplet combination.

Cell lines	Cisplatin [mg mL^{-1}] (±SEM)[a)]	Doxorubicin [ng mL^{-1}] (±SEM)	Methotrexate [ng mL^{-1}] (±SEM)
MG-63	0.25 ± 0.04	13.93 ± 0.37	16.85 ± 0.64
HOS-143B	1.03 ± 0.08	6.53 ± 0.09	28.23 ± 2.05
–	–	–	–
MG-63 (TRI)	0.0181 ± 0.001	3.98 ± 0.34	1.45 ± 0.13
HOS-143 (TRI)	0.0108 ± 0.001	5.89 ± 0.53	0.85 ± 0.07

[a)]SEM = standard error of mean, $n = 3$. TRI = cell lines treated with combination of drugs within single cytotoxicity assay.

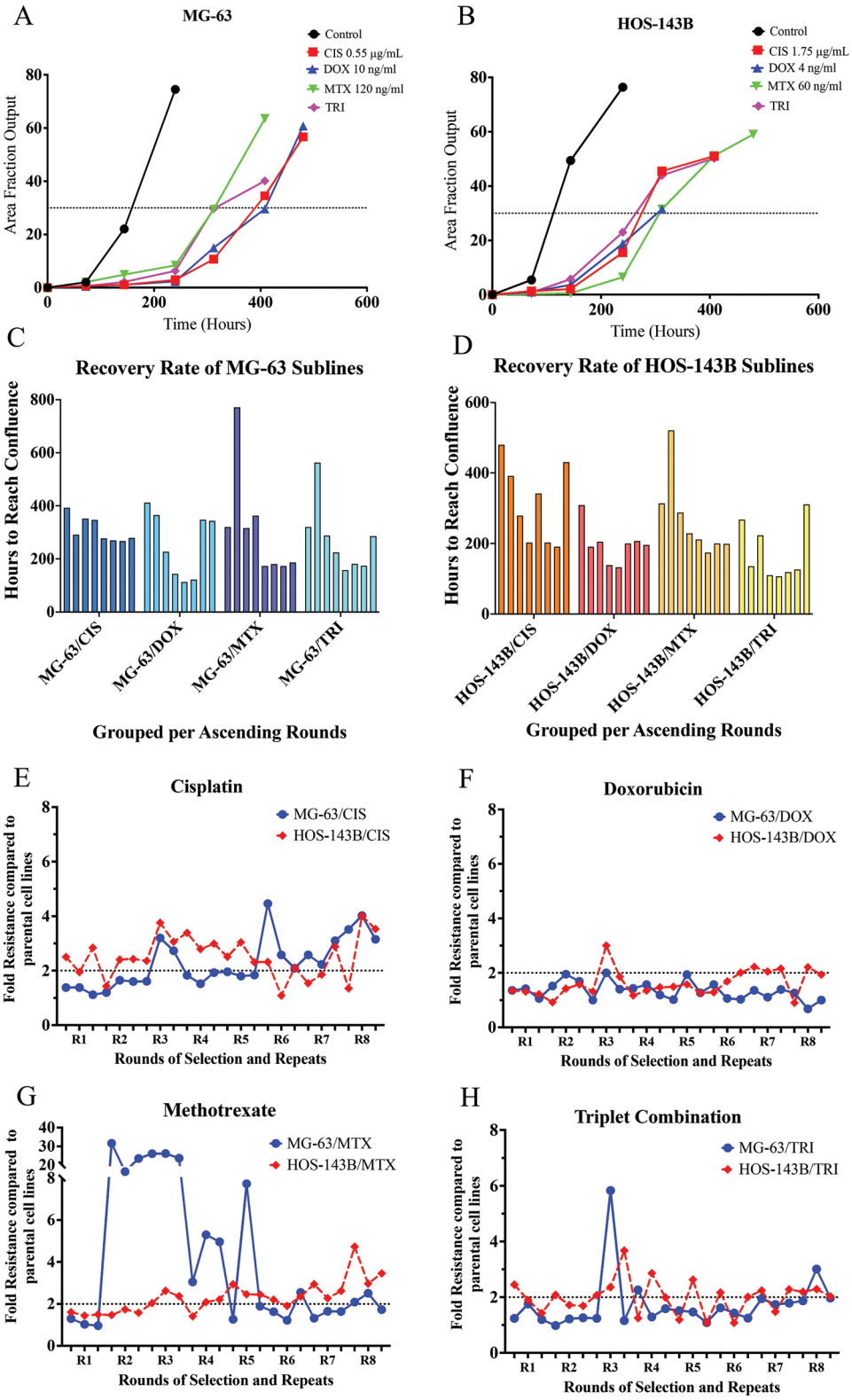

Figure 1. Selection strategy recovery and fold resistance to cisplatin, doxorubicin, methotrexate, and triple-combination of drugs compared to parental cell lines. Recovery is indicated by hours to reach AF output 30 shown on *y*-axis. A) Recovery plot with selected doses for MG-63. B) Recovery plot with selected doses for HOS-143B. C) Recovery plot for MG-63 sublines grouped per ascending round of selection (1–8). D) Recovery plot for HOS-143B sublines grouped per ascending round of selection (1–8). Fold resistance to E) cisplatin, F) doxorubicin, G) methotrexate, and H) triple-combination of drugs is given from round 1–8. The *x*-axis gives a time progression for three weekly cytotoxicity assays in eight rounds of selection. The *y*-axis indicates fold resistance compared to parental cells. Dotted line at twofold indicates the level of clinically relevant drug resistance. The selection strategy was performed once ($n = 1$).

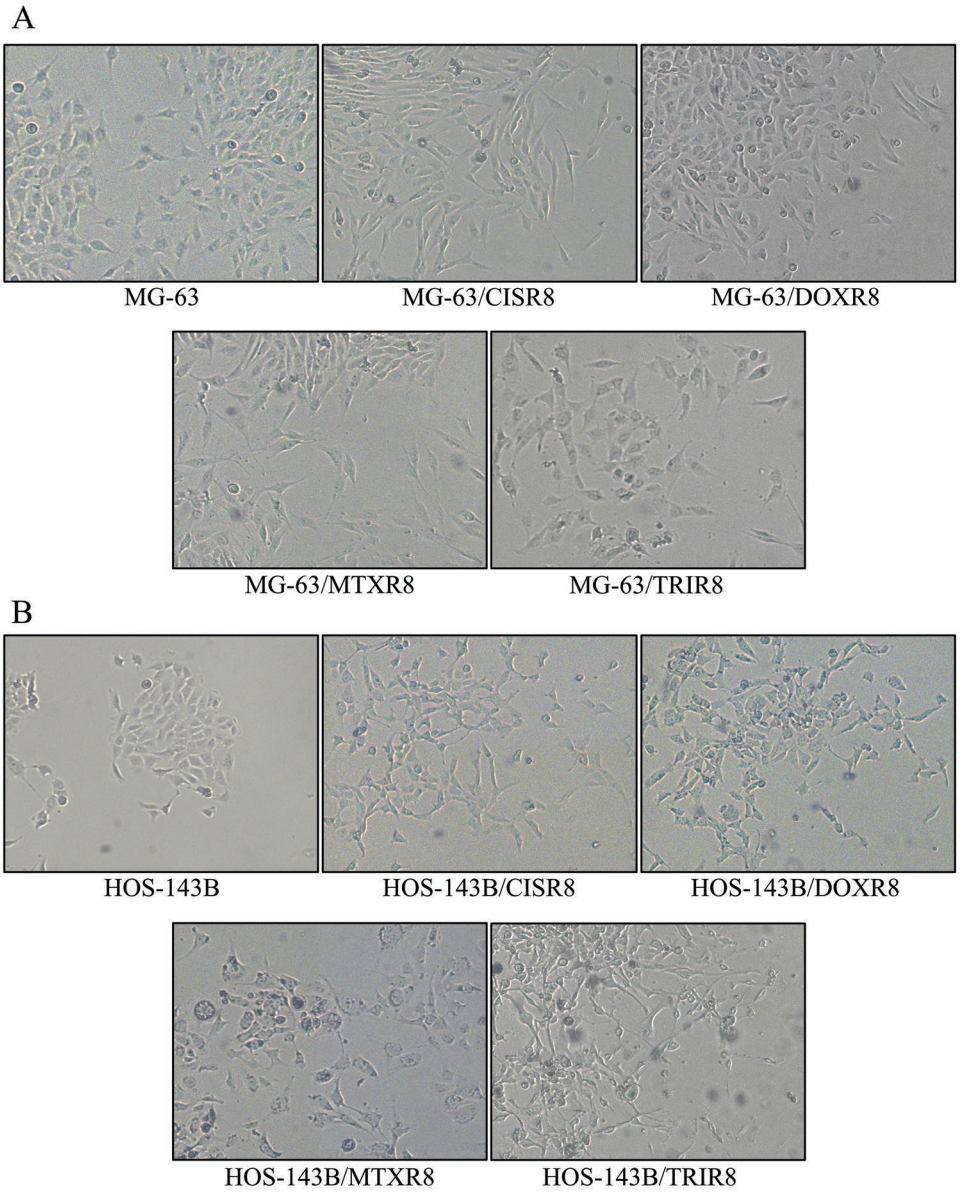

Figure 2. Cell morphology of parental and resistant models of MG-63 and HOS-143B. Cell morphology images were taken by light microscopy at 20× magnification for parental and resistant models of A) MG-63 and B) HOS-143B.

a more elongated spindle like shape. This effect was most pronounced in the cisplatin-resistant models (Figure 3C,D).

2.6. Cross Resistance

A drug screen was performed to evaluate cross resistance to other drugs and to help elucidate resistance mechanisms that had developed in the cells. The cell models were significantly resistant to the agent they were developed with (**Table 2**). Apart from this, the only model that showed a significant cross resistance was MG-63/DOXR8 to cisplatin at 1.88 ± 0.14-fold, p = 0.047. However, some of the resistant models were showing an increase in sensitivity to other chemotherapeutic agents (Table 2). Resistant models developed with combination of drugs (MG-63/TRIR8 & HOS-143B/TRIR8) showed no significant increased or decreased fold resistance to the chemotherapeutic drugs individually.

2.7. Migration and Invasion Rate of Resistant Models

The migration rate of MG-63/CISR8, MG-63/MTXR8, and MG-63/TRIR8 were significantly increased by 2.12 ± 0.33-fold (p = 0.015), 2.55 ± 0.42-fold (p = 0.009), and 2.46 ± 0.16-fold (p = 0.002), respectively (**Figure 4**A). In contrast, migration of HOS-143B/MTXR8 and HOS-143B/TRIR8 was significantly decreased with 0.43 ± 0.20-fold (p = 0.003) and 0.39 ± 0.19-fold

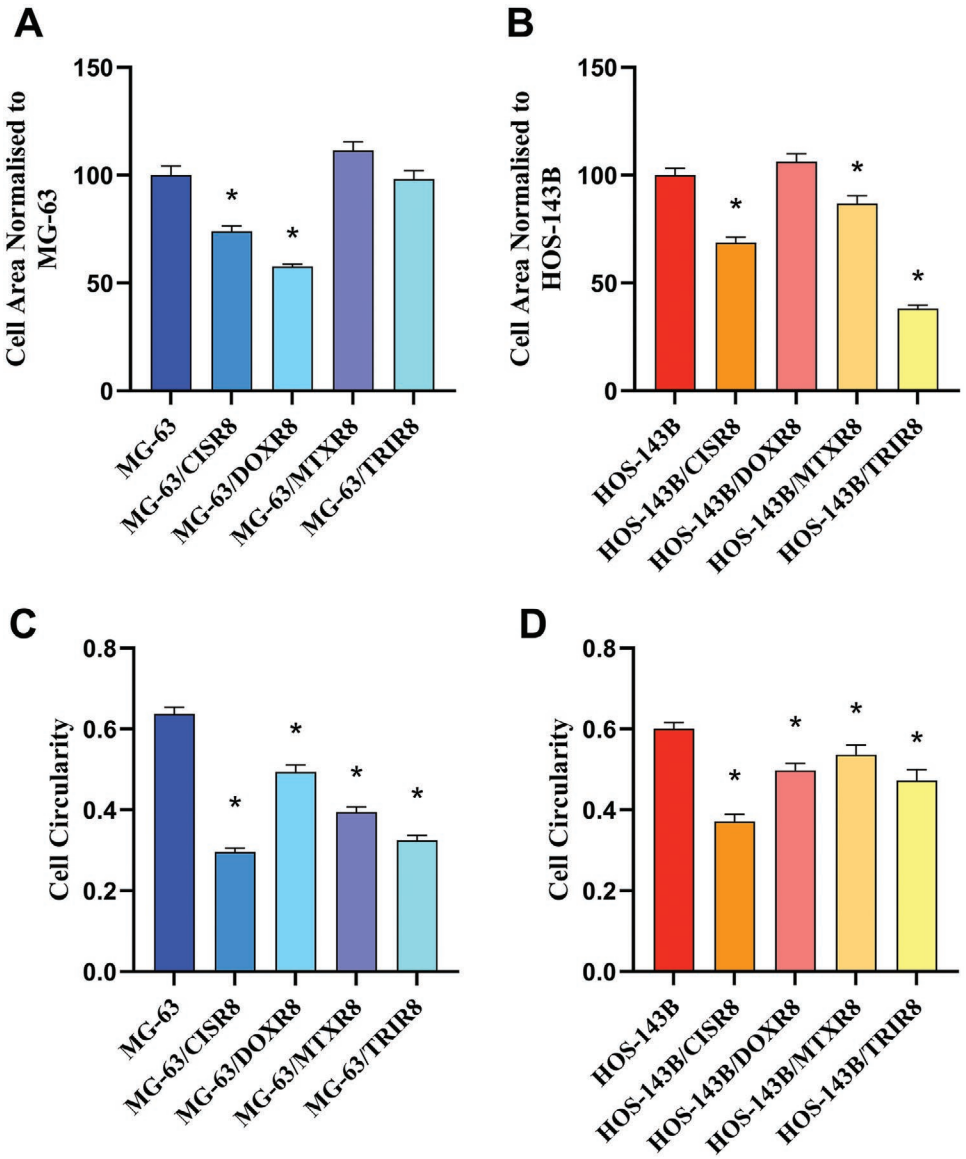

Figure 3. Cell area and circularity. A) Area MG-63 sublines. B) Area HOS-143B sublines. C) Circularity MG-63 sublines. D) Circularity HOS-143B sublines. Analysis was performed on images round 8 of selection, capturing a minimum of 60 cells per image. * Indicated significant difference from parental cell line MG-63 and HOS-143B. $p < 0.05$ Student's *t*-test.

($p = 0.004$) (Figure 4B) . Similar results were also obtained from the invasion assay as MG-63 resistant models were showing a trend for increased invasion and decreased for HOS-143B resistant models. (Figure 4C,D). The invasion rate of MG-63/DOXR8 was significantly increased by 1.78 ± 0.25 ($p = 0.012$) and HOS-143B/DOXR8 was significantly decreased by 0.35 ± 0.03-fold ($p = 0.032$).

2.8. Expression of EMT Genes in Resistant Models

EMT genes were investigated due to the observed alteration of migration and invasion rates in the resistant models. Overall, MG-63 resistant models were showing a trend in decreasing expression level of E-CAD and increasing trend in expression level of mesenchymal marker N-CAD compared to the parental control (Figure 4E). In contrast, HOS-143B resistant models were showing a trend in increasing expression level of epithelial marker E-CAD and a trend in decreasing expression level of N-CAD compared to the parental control (Figure 4F). A significantly decreased E-CAD expression level was determined in MG-63/CISR8 and MG-63/DOXR8 with 0.36 ± 0.15-fold ($p = 0.018$) and 0.36 ± 0.07-fold ($p = 0.005$) and significantly increased N-CAD determined in MG-63/MTXR8 with 2.11 ± 0.18-fold ($p = 0.026$). HOS-143B/CISR8 was showing significantly increased expression level of E-CAD with 1.61 ± 0.14-fold ($p = 0.047$) and significantly decreased N-CAD expression level in HOS-143B/MTXR8 and HOS-143B/TRIR8 with 0.49 ± 0.09-fold ($p = 0.03$)

Table 2. IC_{50} values and fold resistance of drug resistant sublines compared to parental cell.

Cell lines	Cisplatin [mg mL^{-1}] (±SEM)[a)]	Fold resistance (±SEM)	Doxorubicin [ng mL^{-1}] (±SEM)	Fold resistance (±SEM)	Methotrexate [ng mL^{-1}] (±SEM)	Fold resistance (±SEM)
MG-63/CISR8	0.67 ± 0.07 **[c)]	3.56 ± 0.43	5.88 ± 2.95	0.66 ± 0.15	8.98 ± 0.87 *[b)]	0.69 ± 0.14
MG-63/DOXR8	0.37 ± 0.06 *[)]	1.88 ± 0.14	9.04 ± 2.12	1.19 ± 0.16	7.65 ± 1.15 *[)]	0.65 ± 0.10
MG-63/MTXR8	0.19 ± 0.05	0.95 ± 0.14	5.11 ± 1.78	0.59 ± 0.06	23.68 ± 5.78 *[)]	2.11 ± 0.39
MG-63/TRIR8	0.20 ± 0.04	1.02 ± 0.16	11.22 ± 2.05	1.37 ± 0.42	22.32 ± 9.82	1.88 ± 0.80
–	–	–	–	–	–	–
HOS-143B/CISR8	1.35 ± 0.34 *[)]	3.51 ± 0.51	3.77 ± 1.97	1.41 ± 0.20	7.96 ± 1.96	0.82 ± 0.03
HOS-143B/DOXR8	0.36 ± 0.11	0.85 ± 0.07	6.79 ± 0.38 *[)]	1.99 ± 0.20	10.73 ± 1.13	1.14 ± 0.18
HOS-143B/MTXR8	0.12 ± 0.01	0.30 ± 0.08	4.39 ± 2.67	1.57 ± 0.31	48.84 ± 21.82 *[)]	3.77 ± 0.90
HOS-143B/TRIR8	0.26 ± 0.08	0.63 ± 0.06	4.80 ± 2.10	1.80 ± 0.16	10.65 ± 0.05	1.15 ± 0.32

[a)]SEM = Standard error of mean, $n = 3$; [b)]$p < 0.05$; [c)]$p < 0.01$; two-sample *t*-tests compared to MG-63 and HOS-143B parental cell line.

and 0.35 ± 0.06-fold ($p = 0.007$), respectively. Protein expression of N-CAD is shown in Figure 4G. A significantly increased N-CAD protein expression was determined in MG-63/DOXR8 and MG-63/MTXR8 with 2.09 ± 0.22-fold ($p = 0.04$) and 2.97 ± 0.58-fold ($p = 0.038$), respectively (Figure 4H). Conversely, a significantly decrease of N-CAD protein expression was determined in HOS-143B/MTXR8 and HOS-143B/TRIR8 with 0.50 ± 0.13-fold ($p = 0.023$) and with 0.34 ± 0.18-fold ($p = 0.007$), respectively (Figure 4I). Protein expression of E-CAD was not detectable in either cell lines using MCF-7 as a positive control. Changes in mesenchymal marker VIM were observed, but these were much smaller in magnitude than the changes in E-CAD and N-CAD (Figure 4E,F). An increase in EMT-related transcription factor ZEB1 was seen in the MG-63 sublines, consistent with the increase in N-CAD (Figure 4E); this was not observed in the HOS-143B sublines, consistent with the decrease in N-CAD (Figure 4F).

2.9. Expression of P-glycoprotein in Resistant Models

The expression level of P-glycoprotein (P-gp) was measured by RT-PCR and Western blot. The ABCB1 gene was examined to determine the mRNA expression of P-gp. MG-63/CISR8, MG-63/DOXR8, and MG-63/TRIR8 all showed a significant increase of ABCB1 mRNA expression level with 23.24 ± 5.07-fold ($p = 0.005$), 6.26 ± 1.16-fold ($p = 0.024$), and 11.84 ± 2.60-fold ($p = 0.026$), respectively. Conversely, MG-63/MTXR8 was significantly decreased with 0.06 ± 0.01-fold ($p = 0.007$) compared to MG-63 (**Figure 5**A). The ABCB1 mRNA expression level was showing a decreasing trend in all of the HOS-143B resistant models and HOS-143B/DOXR8 was determined to have significantly decreased with 0.32 ± 0.05-fold ($p = 0.01$) compared to HOS-143B (Figure 5B). P-glycoprotein protein expression level was increased in all MG-63 and HOS-143B resistant models except for MG-63/MTXR8 and HOS-143B/MTXR8 as shown in Figure 5C. HOS-143B/CISR8 exhibited significant increase of P-gp protein with 7.74 ± 0.45-fold ($p = 0.02$), followed by HOS-143B/DOXR8 with 3.56 ± 0.49-fold ($p = 0.011$), and HOS-143B/TRIR8 with 2.76 ± 0.52-fold ($p = 0.033$), compared to parental control HOS-143B (Figure 5D).

2.10. Effect of Elacridar Inhibitor on Osteosarcoma Resistant Models

The inhibitor elacridar was used to investigate the reversal of P-gp-mediated drug efflux to enhance the cytotoxicity. Unexpectedly, the combination of elacridar and cisplatin resulted in an increasing IC_{50} value of cisplatin, increasing resistance in MG-63 (2.71 ± 0.13-fold, $p = 0.0001$), MG-63/MTXR8 (1.67 ± 0.06-fold, $p = 0.028$), and MG-63/TRIR8 (2.1 ± 0.31-fold, $p = 0.02$) (**Figure 6**A). However, a significant decrease of IC_{50} value of cisplatin was shown on HOS-143B/CISR8 (0.43 ± 0.07-fold, $p = 0.021$) (Figure 6B). The combination of elacridar and doxorubicin demonstrated a significantly decreased IC_{50} value, reversal of resistance, in MG-63/DOXR8 (0.36 ± 0.06-fold, $p = 0.003$), MG-63/TRIR8 (0.72 ± 0.07-fold, $p = 0.04$), HOS-143B/CISR8 (0.47 ± 0.09-fold, $p = 0.009$), and HOS-143B/TRI (0.45 ± 0.03-fold, $p = 0.0005$) (Figure 6C,D).

2.11. Apoptosis Assay

Percentage of apoptotic cells was determined in the parental and resistant sublines of MG-63 and HOS-143B to investigate the chemotherapeutic drugs induced apoptotic events in the cells. After cisplatin incubation, a significant decrease of apoptotic cells was determined in HOS-143B/CISR8 with EA = 1.39 ± 0.03% ($p = 0.037$) and LA = 7.68 ± 0.22% ($p = 0.014$) compared to HOS-143B (Figure 6E). However, HOS-143B/TRIR8 was showing a significant increase in percentage of apoptotic cells with EA = 11.08 ± 1.57% ($p = 0.049$) and LA = 27.01 ± 1.42% ($p = 0.008$) compared to HOS-143B (Figure 6E). A significant decrease of late apoptotic cells was also determined on MG-63/CISR8 with LA = 10.92 ± 0.46% ($p = 0.023$) compared to MG-63 (Figure 6E). For doxorubicin induced apoptosis, significant decrease of percentage of apoptotic cells was found in HOS-143B/DOXR8 with EA = 1.78 ± 0.08% ($p = 0.032$) and LA = 6.36 ± 0.04% ($p = 0.036$), and HOS-143B/TRI with EA = 1.34 ± 0.04% ($p = 0.02$) and LA = 6.19 ± 0.16 ($p = 0.034$), compared to HOS-143B (Figure 6F). However, MG-63/DOXR8 and MG-63/TRIR8 demonstrated an increased trend compared to parental control MG-63. For methotrexate induced apoptosis, MG-63/MTXR8

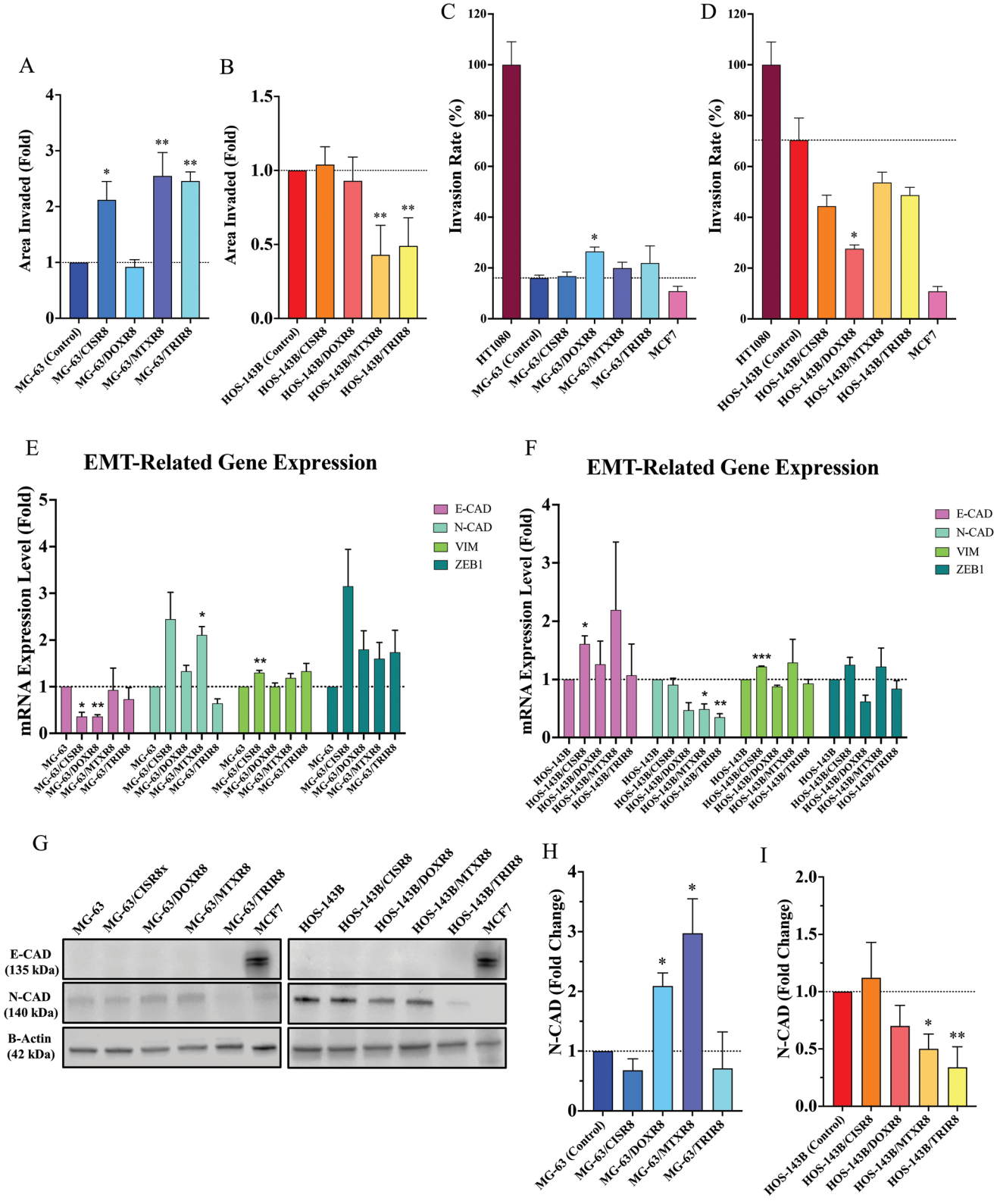

Figure 4. A,B) Wound healing assay and C,D) invasion assay of MG-63 and HOS-143B resistant sublines. Wound healing assay was indicated by the area invaded after 16 h in biological triplicate. HT1080 was used as a positive control and MCF7 as a negative control. EMT-related expression (ZEB1, VIM, E-CAD, and N-CAD). Gene expression determined using RT-qPCR in E) MG-63 and F) HOS-143B resistant sublines. G) Protein expression of N-CAD and the fold change determined in H) MG-63 and I) HOS-143B resistant sublines. MCF7 was used as positive control for E-CAD. Error bars represent SEM. * = $p < 0.05$, ** = $p < 0.01$. Two-sample *t*-tests compared to MG-63 and HOS-143B parental cell line (A–D). One sample *t*-test with hypothesised mean = 1. ($n = 3$) (E–I).

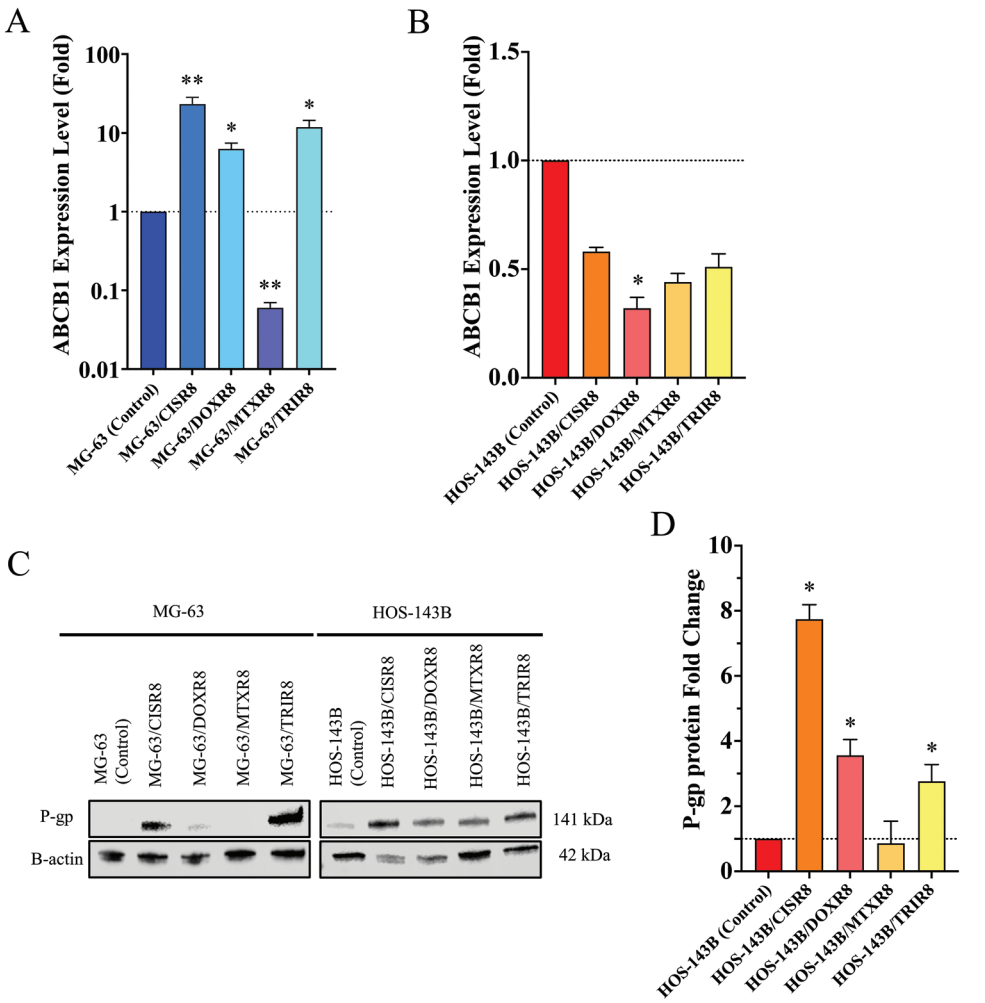

Figure 5. ABCB1 mRNA expression level for A) MG-63 resistant cell lines and B) HOS-143B resistant cell lines analyzed by RT-PCR ($n = 3$). C) P-glycoprotein expression level for MG-63 and HOS-143B resistant cell lines analyzed by Western Blot ($n = 3$). D) Quantitative analysis of P-glycoprotein Western Blots normalising to HOS-143B Control. Error bars represent SEM. * = $p < 0.05$, ** = $p < 0.01$. Two-sample *t*-tests compared to MG-63 and HOS-143B parental cell line.

and MG-63/TRIR8 were showing a significantly decrease in the percentage of late apoptotic cells with 8.07 ± 0.41% ($p = 0.015$) and 13.60 ± 0.95% ($p = 0.037$), respectively. Furthermore, a significant decrease was also determined on the percentage of early apoptotic cells of HOS-143B/MTX and HOS-143B/TRIR8 with EA = 15.24 ± 0.90% ($p = 0.002$) and EA = 14.58 ± 0.21% ($p = 0.002$) accordingly, compared to HOS-143B (Figure 6G).

3. Discussion

3.1. A Pulsed Selection Strategy is the Most Clinically Relevant

In general, there are two selection strategies that can be used in developing drug resistant models: a pulsed or continuous exposure strategy.[27] Drug resistant osteosarcoma models have frequently been developed by increasing the dose of a continuous exposure to the cells.[19,21,22,28] However, osteosarcoma patients normally receive chemotherapeutic drug infusions every 3 to 4 weeks.[29] In the EURAMOS-1 protocol, cisplatin and doxorubicin are first administered simultaneously, and methotrexate is given after 3 weeks.[30] In other protocols such as from Italian Sarcoma Group (ISG/OS-1), cisplatin, doxorubicin, and methotrexate are given as single agents, once each week.[31] To simplify the replication of these different protocols used in different regions in our study, osteosarcoma cells were exposed to a combination of all three chemotherapeutic drugs for a 3-days pulse and allowed to recover in drug-free media for a subsequent 3-weeks until the next dose was given.

The concentration of drugs used in selection was vital in developing a clinically relevant resistant model. To translate the dosage used in clinical treatment to practical use in laboratory, pharmacokinetic studies of cisplatin,[32] doxorubicin,[33] and methotrexate[34] were used as references. The optimized drug doses used in this study fall within the range of concentration determined in the patient's body after intravenous administration.[32–34] The drug concentrations used in this study remain constant throughout the eight rounds of selection as cancer

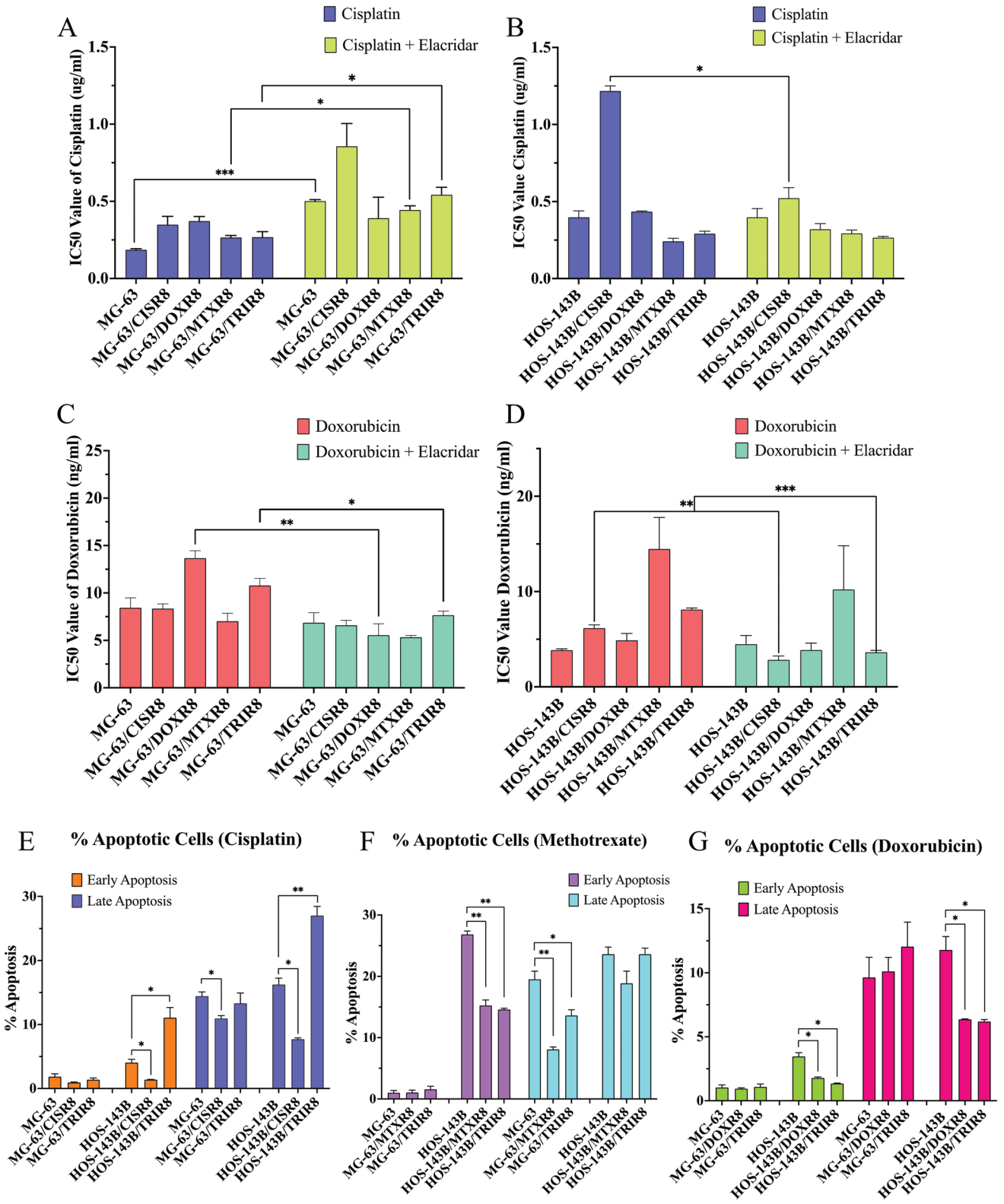

Figure 6. Effect of elacridar on resistant models and the percentage of early and late apoptotic cells after 24 h of incubation with drugs. IC_{50} value of cisplatin with and without elacridar for parental and resistant sublines of A) MG-63 and B) HOS-143B. IC_{50} value of doxorubicin with and without elacridar for parental and resistant sublines of C) MG-63 and D) HOS-143B. Apoptotic cells percentage of MG-63 and HOS-143B parental and resistant sublines after incubation with E) cisplatin (MG-63: 190 ng mL^{-1}; HOS-143B: 380 ng mL^{-1}), F) doxorubicin (MG-63: 5.44 ng mL^{-1}; HOS-143B: 10.87 ng mL^{-1}), and G) methotrexate (MG-63: 11.16 ng mL^{-1}; HOS-143B: 12.56 ng mL^{-1}). Error bars represent SEM. * = $p < 0.05$, ** = $p < 0.01$, *** = $p < 0.001$. Two-sample *t*-tests compared to MG-63 and HOS-143B parental cell line. ($n = 3$).

patients in general do not experience escalating doses of drug. Patients are more likely to have their doses decreased due to unwanted side effects and toxicities.[5,35] In this study, all the developed resistant models were cultured in drug-free media after the completion of the drug selection and the fold resistance was maintained up to 3 months (9 passages). The irreversible resistance observed in these resistant models suggests the alteration of genetic or DNA mutation caused the resistant models in acquiring the resistance.[36]

3.2. Triple-Resistant Models Remain Sensitive to Cisplatin, Doxorubicin, and Methotrexate

Previous osteosarcoma resistant models were developed using single agents only.[19,21,22,37] The objective of this study was to establish resistant osteosarcoma models by using the multiple chemotherapeutic drugs used as standard treatment.[5] Triple-combination osteosarcoma-resistant models, MG-63/TRIR8, and HOS-143B/TRIR8 were established by introducing cisplatin, doxorubicin, and methotrexate simultaneously. Single-agent resistant models were also established. After eight rounds of selection, the fold resistance acquired in the multi-agent osteosarcoma resistant models (MG-63/TRIR8 and HOS-143B/TRIR8) was lower compared to the single-agent resistant models. The drug concentrations used to establish the single-agent models were relatively higher compared to multi-agent models. This was due to the cytotoxicity effect of multiple drugs not being as tolerable in the osteosarcoma cells. This might be responsible for the lower fold resistance acquired in the multi-agent resistant models than the single-agent resistant models.

We hypothesized that the triplet-combination sublines acquired the resistance from cisplatin, doxorubicin, or methotrexate or a combination. However, when a drug screen was performed with the individual drugs separately, MG-63/TRIR8 and HOS-143B/TRIR8 did not show any significant fold resistance to any of the drugs (Table 2). This indicates that a different resistance mechanism was developed within these triple-combination models. When a single agent was given to these triplet-resistant cells, the resistance mechanisms of the single agent were not fully established yet due to lower concentration administrated during the development process; and thus, the sensitivity of these resistant cells toward the single agents remained.

Amongst the MG-63 single-agent resistant model, only MG-63/DOXR8 displayed cross resistance to cisplatin (Table 2). A contrary result was shown by Oda et. Al; their doxorubicin-resistant variants were cross resistant to vincristine but not to cisplatin or methotrexate.[21] Han et. al also found their cisplatin-resistant variant exhibiting cross resistance to methotrexate and doxorubicin.[19] Both studies were conducted by employing an incremental continuous strategy,[19,21] which demonstrates that different mechanisms of resistance can be produced based on the different strategies used.

After drug treatment, percentage of early and late apoptotic cells of the single-agent resistant models of MG-63 and HOS-143B was significantly lower compared to parental controls, confirming their drug resistant status (Figure 6E–G). The exception to this was MG-63/DOXR8, but this was expected as this subline had not acquired any significant fold resistance compared to the parental cell line (Table 2). For the multi-agent induced sublines, a different trend of percentage of apoptosis was seen with different chemotherapeutic drugs. MG-63/TRIR8 demonstrated lower percentage of early and late apoptotic cells compared to parental control MG-63. A similar result was also seen with methotrexate (Figure 6G). However, the percentage of apoptotic cells in response to doxorubicin was the highest in MG-63/TRIR8 compared to MG-63. This indicates that the resistance acquired in MG-63/TRIR8 was contributed mainly from the resistant mechanism of cisplatin and methotrexate instead of doxorubicin. For HOS-143B/TRIR8, the percentage of early and late apoptotic cells were significantly lower than parental HOS-143B after the exposure of doxorubicin and methotrexate drug. This suggests the acquired resistance in HOS-143B/TRIR8 on the combination of drugs was largely contributed from the resistance mechanism of doxorubicin and methotrexate instead of cisplatin. The Bcl-2 family that is responsible for regulating programmed cell death pathway[38] could play an important role in these resistant models as it had demonstrated to be a potent suppressor of programmed cell death in response to chemotherapy.[39]

The original IC_{50} values suggest that MG-63 was initially more sensitive to cisplatin and methotrexate compared to HOS-143B, and HOS-143B was originally more sensitive to doxorubicin compared to MG-63 (Table 1). After multiple rounds of treatment with the combination of drugs, even though no resistance was seen in the multi-agent resistant models to single drugs, the osteosarcoma cells appeared to acquire their resistance mechanisms based on their most sensitive drug. Both of the triplet-resistant osteosarcoma cell lines acquired methotrexate resistance mechanisms and then the mechanism of their most sensitive drugs, either cisplatin or doxorubicin. Therefore, the resistance of MG-63/TRIR8 was determined to be compensated more from cisplatin and methotrexate resistant mechanisms, while HOS-143B/TRIR8 was complimented largely from doxorubicin and methotrexate according to the apoptosis results (Figure 6E–G).

3.3. P-glycoprotein Mediates Resistance to Doxorubicin and is a Stress Response to Cisplatin

P-glycoprotein (P-gp) is responsible for one of the well-established causes of drug resistance in cancer cells.[40] In this study, P-gp protein was overexpressed in all the resistant models developed from MG-63 and HOS-143B except for the resistant models established by methotrexate as a single-agent (MG-63/MTXR8 & HOS-143B/MTXR8). The overexpression of P-gp in cisplatin treated cancer models was investigated in ovarian cancer cell line by Stordal et al., demonstrating that this was a representation of a generalized stress response as cisplatin is not a P-gp substrate.[41]

A meta-analysis study on osteosarcoma from Liu et al. involved 11 studies conducted between 1995 and 2016 with a total of 723 participants from different territories and showed that the higher expression of P-gp may predict poorer survival. Sensitivity of the doxorubicin resistant osteosarcoma cell line KHOSR2 to doxorubicin was restored with the knockout

of ABCB1 by CRIPSR-Cas9.[18] Our study also demonstrated a similar result as the sensitivity of MG-63/DOXR8, MG-63/TRIR8, HOS-143B/CISR8, and HOS-143B/TRIR8 to doxorubicin was restored when the P-gp was inhibited by elacridar (Figure 6C,D). However, the inhibition of P-gp by elacridar had not increased the sensitivity of MG-63 resistant sublines to cisplatin but had increased the resistance to cisplatin instead (Figure 6A). Furthermore, this again has suggested cisplatin was not a substrate of P-gp; and therefore, sensitivity of cisplatin was not restored.[41] Nonetheless, the sensitivity of HOS-143B/CISR8 to cisplatin was restored by the inhibition of P-gp as shown in Figure 6B. A study from Ali et al. obtained a similar result as their lung-cancer resistant variants H23/CPR and H2126/CPR were showing significantly increased sensitivity to cisplatin when exposed to elacridar.[42] Inhibiting the P-gp transporter had a sensitization effect on the cisplatin resistance models; however, it was not directly associated to the transport action of P-gp as cisplatin is not a substrate.[41] Furthermore, the expression of P-gp could also be modulated by the formation of reactive oxygen species (ROS), which are produced in the response to cisplatin.[43] As doxorubicin also generates free radical-mediated oxidative damage,[40] this may be the mechanisms of P-gp upregulation in the cisplatin and doxorubicin induced resistant models.

3.4. Drug Resistance is Associated With EMT or MET Signaling in Osteosarcoma Cells

We investigated the migration and invasion rate on these resistant models compared to their respective parental control. Figure 4A shows the migration rate of MG-63/CISR8, MG-63/MTXR8, and MG-63/TRIR8 was significantly increased, and an increasing trend of invasion rate was also determined on MG-63 resistant models compared to the parental control (Figure 4C). The EMT biomarkers gene expression of the MG-63 resistant models was showing an increasing trend of N-CAD and decreasing of E-CAD (Figure 4E). Decreasing levels of E-cadherin lead to the activation of several EMT transcription factors and result in increasing invasion and metastasis;[44,45] therefore, promoting the migration and invasion rate of MG-63 resistant models.

Conversely, the HOS-143B resistant models showed the opposite result in the gene expression of EMT biomarkers; E-CAD was showing an increasing trend and N-CAD, a decreasing trend (Figure 4F). This indicates that the HOS-143B underwent mesenchymal to epithelial transition (MET) instead of EMT. E-CAD and N-CAD are known as the "cadherin switch" to expressing in the opposite trend to each other to regulate the progression of EMT or MET.[46] With the HOS-143B resistant models transited from a mesenchymal cell type to a more epithelial phenotype, the migration and invasion rate of these models were also significantly decreased compared to parental control (Figure 4B,D). Our cell morphology analysis is supportive of a switch to an EMT state in the MG-63 resistant models, with a shift to a more spindle-like morphology as shown by a decrease in circularity (Figures 2 and 3). The HOS-143B models also show a decrease in circularity, the opposite of what would be suggested by an increase in MET signaling.

The plasticity event of EMT/MET processes is believed to be involved in the activation of tumor metastasis, where EMT activation promotes tumor cells dissemination and invasion from primary tumor site and MET activation to support metastatic outgrowth in distant organs.[47] The distinctive activation of EMT and MET from these two resistant model cell lines could demonstrate a different state of metastasis. MG-63 resistant models with the activation of EMT could represent the primary tumor cells gradually disseminating, and HOS-143B resistant models are the tumor cells arriving in distant organs.

4. Conclusion

In summary, resistance in osteosarcoma cells appears to induce an EMT switch in the cells with a lower degree of metastasis (MG-63) but the reverse (MET) in the highly metastatic osteosarcoma cells (HOS-143B). Drug resistance in osteosarcoma cells; is therefore, not always associated with increased migration and invasion. Drug resistance is also associated with P-gp expression, but this may be a generic stress response as elacridar is not able to consistently sensitize the resistant models. The multi-agent resistant models MG-63/TRIR8 and HOS-143B/TRIR8 do not show any resistance to the single-agent drugs. However, the resistance mechanism of MG-63/TRIR8 is determined to be primarily from cisplatin and methotrexate, while HOS-143B/TRIR8 are largely from doxorubicin and methotrexate.

5. Experimental Section

Cell Culture: Osteosarcoma cell lines MG-63 and HOS-143B were grown in DMEM supplemented with 10% fetal calf serum, 1% sodium pyruvate, and 1% non-essential amino acids (NEAA) free of antibiotics (All from Gibco, Thermo Fisher Scientific). MCF7 was grown in DMEM supplemented with 10% fetal calf serum (Gibco, Thermo Fisher Scientific) and used as positive control for E-Cadherin on Western blot. Cells were maintained in a humidified atmosphere of 5% CO_2 at 37 °C. Cells at log phase of growth were used in the experiments. Cell lines were routinely checked for mycoplasma and were mycoplasma-free.[48]

Cell Selection Strategy Outline: MG-63 and HOS-143B were treated with cisplatin (St. James Hospital pharmacy), doxorubicin (Sigma–Aldrich), methotrexate (Sigma–Aldrich), or a triplet combination of drugs into different resistance sublines. The format of the sublines was named in the format of "Parental cell line/Treatment and Round." The drug treatment was termed as "CIS" (cisplatin), "DOX" (doxorubicin), "MTX" (methotrexate), or "TRI" (combination of cisplatin, doxorubicin, and methotrexate), and the round of treatment was designated values from "1" to "8". All sublines had a recovery period of 4–5 weeks before the next round of treatment was proceeded.

2.6×10^4 cells were plated into T-25flasks in 5 mL of complete media and allowed to attach overnight. For MG-63, the single-agent treatment used for cisplatin was 0.55 μg mL^{-1}, doxorubicin was 0.01 μg mL^{-1}, and methotrexate was 0.12 μg mL^{-1}; while concentrations used for the triple-combination treatment were 0.05, 0.004, and 0.004 μg mL^{-1}, respectively. For HOS-143B, single-agent treatment used for cisplatin was 1.75 μg mL^{-1}, doxorubicin was 0.004 μg mL^{-1}, and methotrexate was 0.002 μg mL^{-1}; while concentrations used for triplet combination of treatment were 0.02, 0.004, and 0.002 μg mL^{-1}, respectively.

Flasks were incubated for 72 hours at 37 °C with 5% CO_2 after treatment. Drugged media was removed and replaced with drug-free media after incubation. Over subsequent days, confluence was

determined using the area fraction output method[49] and the confluency was determined by using ImageJ software.[50] Cytotoxicity assays were performed once a week for 3 weeks. The fold resistance was calculated by comparing cytotoxicity at each time point with the parental cell line. The next round of treatment commenced once all the cell lines had recovered.

Morphology Analysis: Images of MG-63 and HOS-143B parental and resistant models were captured at 20× magnification and saved as a tif file. Images of the cells were analyzed using ImageJ software.[51] A minimum of 60 cells per image were manually outlined and then analyzed for cell size and circularity.

Cytotoxicity Assays: The sensitivity of the cells to chemotherapy drugs was determined by acid phosphatase assay.[27] The cells were plated into 96-well plates at a cell density of 1×10^3 cells per well and allowed to attach overnight. Serial dilutions of drugs were used to treat the wells in triplicate in a final volume of 200 µL. The highest drug concentration used for single-agent cisplatin was 2.5 µg mL^{-1}, doxorubicin was 0.5 µg mL^{-1}, and methotrexate was 200 ng mL^{-1}. The combination was optimized from the highest drug concentration used in single-agent cytotoxicity assay. The final highest concentrations used for the triplet drug combination were cisplatin at 0.25 µg mL^{-1}, doxorubicin 0.05 µg mL^{-1}, and methotrexate 20 ng mL^{-1}. Elacridar (Sigma–Aldrich) was added to the wells prior to the introductions of serial dilutions of drugs and were incubated overnight with the concentration of 2.5 µM for HOS-143B resistant models and 5 µM for MG-63 resistant models.[52] Drug-free controls were added with 100 µL of fresh complete medium. Cells were then incubated for 5 days at 37 °C in 5% CO_2 and an acid phosphatase assay was used to determine cell viability.[53] On day 5, the media were discarded from the wells and washed twice with PBS. Concentration of 2.63 mg mL^{-1} of phosphatase substrate (Sigma–Aldrich) was dissolved in sodium acetate buffer and 100 µL was added to each well. After incubating the plate at 37 °C for an hour, 50 µL of 1 M sodium hydroxide was added and the absorbance was measured at 405 nm on the plate reader (Omega FLUOStar, BMG Labtech).

Wound Healing Assay: 3×10^4 cells were seeded into a 24-well plate to create a confluent monolayer. The monolayer was "scratched" in a straight line with a p200 pipette tip. Debris was removed by washing once with 1 mL of PBS and replaced with 1 mL of complete medium. Markings were created to be used as a reference point close to the scratch on the outer bottom of the plate to obtain the same field during the image acquisition. Images were taken using a phase-contrast microscope and after initial scratch (T0) and again after 16 h incubation at 37 °C in 5% CO2. The area and length of uninvaded space within each well were measured using ImageJ at T0 and T16.[51,54]

Transwell Assay: 96-well Transwell inserts (Corning, 8 µm pore size) were used for the invasion assay. Cells were pre-labelled with DilC12(3) perchlorate (10 ug mL^{-1}) (Sigma–Aldrich) for 2 h. Next, extracellular matrix (ECM) gel was prepared with the following components: – Collagen IV (Sigma–Aldrich, 100 µg mL^{-1}), Fibronectin (Sigma–Aldrich, 11.4 µg mL^{-1}), Laminin (Sigma–Aldrich, 11.4 µg mL^{-1}), and Collagen I (ThermoFisher, 100 µg mL^{-1}), in serum-free medium and neutralized to pH 7.4 using 0.5 N Sodium hydroxide (NaOH). ECM gel (25 µL per well) was then added onto the insert wells and incubated at 37 °C for 2 h. 4×10^5 cells per mL was prepared in serum-free DMEM and seeded in the top chamber, and 170 uL medium containing 10% FBS was placed into the lower chamber as a chemoattractant. After 24 h of incubation at 37 °C with 5% of CO_2, the cells on the upper membrane surface were removed using a cotton swab and the invading cells were measured using fluorescence (549/565 nm; Ex/Em). HT1080 and MCF7 cell lines were used as positive and negative control for the invasion assay.[55]

RT-PCR: Total RNA was isolated from cells using PureLink RNA Mini kit (Invitrogen; Thermo Fisher Scientific). RNA was then reverse transcribed to cDNA by using SuperScript IV Reverse Transcriptase (Invitrogen, Thermo Fisher Scientific) and 1 µg total RNA. Quantitative real-time PCR (RT-qPCR) was then performed to detect gene expression using TaqMan Gene Expression Assay (Applied Biosystems, Thermo Fisher Scientific) on the LightCycler 96 (Roche). The thermo cycling conditions were as follows: initial denaturation and polymerase activation at 95 °C for 10 min, 40 cycles of denaturation at 95 °C for 15 s, and annealing and extension at 60 °C for 60 s, using instrument default settings for melt curve analysis. The expression of the gene of interest was normalized to GAPDH. The data were then analyzed by using the ΔΔCq method.[56]

Western Blots: Total proteins were extracted with RIPA buffer (Thermo Fisher Scientific). The concentration of protein was determined by the Bradford Assay (Sigma–Aldrich). Western blot was performed according to the method of Stordal et al.[41] Primary antibodies (Rabbit monoclonal anti-Pgp antibody, Abcam; Rabbit monoclonal anti-N-CAD, Cell Signaling Technology; Rabbit monoclonal anti-E-CAD, Cell Signaling Technology) were incubated at 1:1000 dilution. Peroxidase-conjugated secondary antibody (Goat Anti-Mouse IgG; Bio-Rad) was incubated at 1:2000 dilution. The bands were visualized by Li-Cor instrument (LI-COR Biosciences) and measured by Image Studio software (version 3.1; Li-COR Biosciences). β-actin (ab8226, Abcam) was developed again in the second developing step following the same procedure for quantification purposes.

Apoptosis Assay: The number of apoptotic cells was determined by using FITC Annexin V (BD Bioscience). 1×10^6 cells per mL of cells was re-suspended in 2 mL media, plated into a 6-wells plate (Sarstedt AG & Co), and incubated at 37 °C with 5% of CO_2 for 24 h. Drugs were then added to the cells, cisplatin 190 ng mL^{-1}, doxorubicin 5.44 ng mL^{-1}, and methotrexate 11.16 ng mL^{-1} for MG-63 and cisplatin 380 µg mL^{-1}, doxorubicin 10.87 ng mL^{-1}, and methotrexate 12.56 ng mL^{-1} for HOS-143B. Cells were trypsinized after 72 h, resuspended, and washed twice with cold PBS. 1 mL of 1′ Annexin V Binding Buffer was added to resuspend the washed cells and 100 µL of the cell suspension was transferred to a Falcon tube. 5 µL of the FITC Annexin V and 5 µL of PI Staining solution (BD Bioscience) were added and incubated at room temperature in the dark for 15 min. Then, 400 µL of the 1′ Annexin V Binding Buffer was added, and the sample analyzed by flow cytometry (BD FACSCalibur, BD Bioscience) within 1 h. The data were analyzed by using the software CellQuest Pro and producing a quadrant analysis.

Statistical Analysis: All experiments were repeated at a minimum in biological triplicate excluding the cell selection strategy. Statistical analysis was performed using Minitab (version 19.2020.1.0) using either a two-sample *t*-test or one-sample *t*-test comparing to a hypothesized mean of 1. Graphs are presented using the mean ± SEM (standard error of the mean) from at least three independent experiments. *P*-values < 0.05 were considered statistically significant. Graphs were produced using GraphPad Prism 8 (GraphPad Software, USA).

Acknowledgements

The authors acknowledge Middlesex University for internal funding.

Conflict of Interest

The authors declare no conflict of interest.

Author Contributions

Performed the laboratory work and wrote the manuscript: K.L. Supervised the work including the data analysis: F.H., H.R., and B.S. All authors read and approved the manuscript and agree to be accountable for all aspects of the research in ensuring that the accuracy or integrity of any part of the work is appropriately investigated and resolved.

Data Availability Statement

The data that support the findings of this study are available in the supplementary material of this article.

Keywords

chemoresistance, cisplatin, doxorubicin, methotrexate, osteosarcoma

Received: July 11, 2022
Revised: October 27, 2022
Published online:

[1] A. Jemal, F. Bray, M. M. Center, J. Ferlay, E. Ward, D. Forman, *CA - Cancer J. Clin.* **2011**, *61*, 69.
[2] J. J. Morrow, I. Bayles, A. P. W. Funnell, T. E. Miller, A. Saiakhova, M. M. Lizardo, C. F. Bartels, M. Y. Kapteijn, S. Hung, A. Mendoza, G. Dhillon, D. R. Chee, J. T. Myers, F. Allen, M. Gambarotti, A. Righi, A. Difeo, B. P. Rubin, A. Y. Huang, P. S. Meltzer, L. J. Helman, P. Picci, H. H. Versteeg, J. A. Stamatoyannopoulos, C. Khanna, P. C. Scacheri, *Nat. Med.* **2018**, *24*, 176.
[3] Y. M. Huang, C. H. Hou, S. M. Hou, R. S Yang, *Clin. Med.: Oncol.* **2009**, *3*, 99.
[4] J. Ritter, B. S. S. Osteosarcoma, *Ann. Oncol.* **2010**, *21*, vii320.
[5] A. Luetke, P. A. Meyers, I. Lewis, H. Juergens, *Cancer Treat. Rev.* **2014**, *40*, 523.
[6] S. Simpson, M. D. Dunning, S. de Brot, L. Grau-Roma, N. P. Mongan, C. S Rutland, *Acta Vet. Scand.* **2017**, *59*, 71.
[7] P. A. Meyers, C. L. Schwartz, M. Krailo, E. S. Kleinerman, D. Betcher, M. L. Bernstein, E. Conrad, W. Ferguson, M. Gebhardt, A. M. Goorin, M. B. Harris, J. Healey, A. Huvos, M. Link, J. Montebello, H. Nadel, M. Nieder, J. Sato, G. Siegal, M. Weiner, R. Wells, L. Wold, R. Womer, H. Grier, *J. Clin. Oncol.* **2005**, *23*, 2004.
[8] L. Kager, A. Zoubek, U. Pötschger, U. Kastner, S. Flege, B. Kempf-Bielack, D. Branscheid, R. Kotz, M. Salzer-Kuntschik, W. Winkelmann, G. Jundt, H. Kabisch, P. Reichardt, H. Jürgens, H. Gadner, S. S. Bielack, *J. Clin. Oncol.* **2003**, *21*, 2011.
[9] P. Chen, W. L. Gu, M. Z. Gong, J. Wang, D. Q Li, *Cell. Physiol. Biochem.* **2017**, *43*, 1939.
[10] K. Scotlandi, P. Picci, H. Kovar, *Curr. Cancer Drug Targets* **2009**, *9*, 843.
[11] P. E. Lønning, S. Knappskog, *Oncogene* **2013**, *32*, 5315.
[12] S. Yamamoto, H. Tsuda, K. Honda, K. Onozato, M. Takano, S. Tamai, I. Imoto, J. Inazawa, T. Yamada, O. Matsubara, *Mod. Pathol.* **2009**, *22*, 499.
[13] Z. Derdak, N. M. Mark, G. Beldi, S. C. Robson, J. R. Wands, G. Baffy, *Cancer Res.* **2008**, *68*, 2813.
[14] W. Zhang, Q. Li, C. Song, L. Lao, *Tumor Biol.* **2015**, *36*, 2531.
[15] A. J. Chou, R. Gorlick, *Expert Rev. Anticancer Ther.* **2006**, *6*, 1075.
[16] M. Susa, A. K. Iyer, K. Ryu, E. Choy, F. J. Hornicek, H. Mankin, L. Milane, M. M. Amiji, Z. Duan, *PLoS One* **2010**, *5*, e10764.
[17] M. M. Gottesman, T. Fojo, S. E Bates, *Nat. Rev. Cancer* **2002**, *2*, 48.
[18] T. Liu, Z. Li, Q. Zhang, K. D. A Bernstein, S. Lozano-Calderon, E. Choy, F. J. Hornicek, Z. Duan, *OncoTargets Ther.* **2016**, *7*, 83502.
[19] T. Han, X. Zhu, J. Wang, H. Zhao, Q. Ma, J. Zhao, X. Qiu, Q. Fan, *Oncol. Rep.* **2014**, *32*, 1133.
[20] B. H. Niu, J. J. Wang, Y. Xi, X. Y Ji, *Med. Sci. Monit.* **2010**, *16*, BR184.
[21] Y. Oda, Y. Matsumoto, K. Harimaya, Y. Iwamoto, M. Tsuneyoshi, *Oncol. Rep.* **2000**, *7*, 859.
[22] J.-q. Yin, J.-n. Shen, W.-w. Su, J. Wang, G. Huang, S. Jin, Q.-c. Guo, C.-y. Zou, H.-m. Li, F.-b. Li, *Acta Pharmacol. Sin.* **2007**, *28*, 712.
[23] C. Pautke, M. Schieker, T. Tischer, *et al.*, *Anticancer Res. Published online* **2004**, *6*, 3743.
[24] H. H. Luu, Q. Kang, J. K. Park, W. Si, Q. Luo, W. Jiang, H. Yin, A. G. Montag, M. A. Simon, T. D. Peabody, R. C. Haydon, C. W. Rinker-Schaeffer, T.-C. He, *Clin. Exp. Metastasis* **2005**, *22*, 319.
[25] A. B. Mohseny, I. Machado, Y. Cai, K.-L. Schaefer, M. Serra, P. C. W. Hogendoorn, A. Llombart-Bosch, A.-M. Cleton-Jansen, *Lab Invest.* **2011**, *91*, 1195.
[26] H. Heremans, A. Billiau, J. J. Cassiman, J. C. Mulier, P. de Somer, *Oncology* **1978**, *35*, 246.
[27] N. Asada, H. Tsuchiya, K. Tomita, *Anticancer Res.* **1999**, *19*, 5131.
[28] M. Mcdermott, A. J. Eustace, S. Busschots, L. Breen, J. Crown, M. Clynes, N. O'Donovan, B. Stordal, *Front Oncol* **2014**, *4*.
[29] A. C. Noël, A. Callé, H. P. Emonard, B. V. Nusgens, L. Simar, J. Foidart, C. M. Lapiere, J. M. Foidart, *Cancer Res.* **1991**, *51*, 405.
[30] D. Carrle, S. S Bielack, *Int. Orthop.* **2006**, *30*, 445.
[31] J. S. Whelan, S. S. Bielack, N. Marina, S. Smeland, G. Jovic, J. M. Hook, M. Krailo, J. Anninga, T. Butterfass-Bahloul, T. Böhling, G. Calaminus, M. Capra, C. Deffenbaugh, C. Dhooge, M. Eriksson, A. M. Flanagan, H. Gelderblom, A. Goorin, R. Gorlick, G. Gosheger, R. J. Grimer, K. S. Hall, K. Helmke, P. C. W. Hogendoorn, G. Jundt, L. Kager, T. Kuehne, C. C. Lau, G. D. Letson, J. Meyer, et al., *Ann. Oncol.* **2015**, *26*, 407.
[32] S. Ferrari, P. Ruggieri, G. Cefalo, A. Tamburini, R. Capanna, F. Fagioli, A. Comandone, R. Bertulli, G. Bisogno, E. Palmerini, M. Alberghini, A. Parafioriti, A. Linari, P. Picci, G. Bacci, *J. Clin. Oncol.* **2012**, *30*, 2112.
[33] S. Bielack, R. Erttmann, G. Looft, C. Purfürst, G. Delling, K. Winkler, G. Landbeck, *Cancer Chemother. Pharmacol.* **1989**, *24*, 376.
[34] D. R. Barpe, D. D. Rosa, P. E Froehlich, *Eur. J. Pharm. Sci.* **2010**, *41*, 458.
[35] K. R. Crews, T. Liu, C. Rodriguez-Galindo, M. Tan, W. H. Meyer, J. C Panetta, M. P. Link, N. C. Daw, *Cancer* **2004**, *100*, 1724.
[36] K. A. Janeway, H. E Grier, *Lancet Oncol.* **2010**, *11*, 670.
[37] R. Salgia, P. Kulkarni, *Trends Cancer* **2018**, *4*, 110.
[38] S. Ferrari, S. Smeland, M. Mercuri, F. Bertoni, A. Longhi, P. Ruggieri, T. A. Alvegard, P. Picci, R. Capanna, G. Bernini, C. Müller, A. Tienghi, T. Wiebe, A. Comandone, T. Böhling, A. B. Del Prever, O. Brosjö, G. Bacci, G. Sæter, *J. Clin. Oncol.* **2005**, *23*, 8845.
[39] J. C Reed, *Oncogene* **1998**, *17*, 3225.
[40] P. P. Ruvolo, X. Deng, W. S May, *Leukemia* **2001**, *15*, 515.
[41] S. Sritharan, N. Sivalingam, *Life Sci.* **2021**, *278*, 119527.
[42] B. Stordal, M. Hamon, V. Mceneaney, S. Roche, J.-P. Gillet, J. J. OâLeary, M. Gottesman, M. Clynes, *PLoS One* **2012**, *7*, e40717.
[43] S. Ali, M. Tahir, A. Khan, X. Chen, M. Ling, Y. Huang, *Iran J. Med. Sci.* **2019**, *20*, 1125.
[44] M. Berndtsson, M. Hägg, T. Panaretakis, A. M. Havelka, M. C. Shoshan, S. Linder, *Int. J. Cancer* **2007**, *120*, 175.
[45] T. T. Onder, P. B. Gupta, S. A. Mani, J. Yang, E. S. Lander, R. A Weinberg, *Cancer Res.* **2008**, *68*, 3645.
[46] G. Yang, J. Yuan, K. Li, *Med. Oncol.* **2013**, *30*, 697.
[47] C.-Y. Loh, J. Chai, T. Tang, W. Wong, G. Sethi, M. Shanmugam, P. Chong, C. Looi, *Cells* **2019**, *8*, 1118.
[48] M. Diepenbruck, G. Christofori, *Curr. Opin. Cell Biol.* **2016**, *43*, 7.
[49] L. Young, J. Sung, G. Stacey, J. R Masters, *Nat. Protoc.* **2010**, *5*, 929.
[50] S. Busschots, S. O'Toole, J. J. O'Leary, B. Stordal, *MethodsX* **2015**, *2*, 8.
[51] C. A. Schneider, W. S. Rasband, K. W Eliceiri, *Nat. Methods* **2012**, *9*, 671.
[52] T. J Collins, *BioTechniques* **2007**, *43*, S25.
[53] D. Lawlor, P. Martin, S. Busschots, J. Thery, J. J. OâLeary, B. T. Hennessy, B. Stordal, *J. Pharm. Sci.* **2014**, *103*, 1913.
[54] T. T. Yang, P. Sinai, S. R Kain, *Anal. Biochem.* **1996**, *241*, 103.
[55] L. G. Rodriguez, X. Wu, J. L Guan, *Methods Mol. Biol.* **2005**, *294*, 23.
[56] K. J. Livak, T. D Schmittgen, *Methods* **2001**, *25*, 402.